AERE - R 5223

UNCLASSIFIED
(Approved for Publication)

AERE - R 5223

United Kingdom Atomic Energy Authority

RESEARCH GROUP

Report

INERT GAS BUBBLES IN NEUTRON IRRADIATED MAGNESIUM OXIDE

C. S. MORGAN D. H. BOWEN

Ceramics Division,

Atomic Energy Research Establishment,

Harwell, Berkshire.

1966

U.D.C.
661.846.22-179
546.291
546.292

UNCLASSIFIED AERE-R 5223
(Approved for Publication)

INERT GAS BUBBLES IN NEUTRON IRRADIATED MAGNESIUM OXIDE

by

C. S. Morgan* and D. H. Bowen

ABSTRACT

In magnesium oxide, irradiated with neutrons at 150°C, 600°C and 1,000°C to doses greater than 10^{20} nvt ⩾ 1 MeV, rectilinear bubbles have been observed by transmission electron microscopy after annealing at temperatures above 1,500°C. The bubbles had {100} surfaces and sides ranging from 40-400 Å and measurements of the residual growth of the crystals after annealing have been correlated with the volume occupied by the bubbles.

Electron microscope and gas release studies indicate that the bubbles form primarily by vacancy condensation and subsequently act as sinks for the diffusion of neon and helium produced by the transmutation of magnesium and oxygen. It is suggested that mechanical release of these gases, by crushing the crystals at room temperature, can take place by two processes; the intersection of bubbles by cracks and by transport of gas via irradiation-induced dislocations.

In a crystal irradiated at 1,000°C, large precipitates were formed that, on annealing, dissolved, leaving behind bubbles up to 2,000 Å in size, having a variety of crystallographic shapes.

*On attachment from:

Metals and Ceramics Division,
Oak Ridge National Laboratory,
Oak Ridge,
Tennessee, U.S.A.

Ceramics Division,
U.K.A.E.A. Research Group,
Atomic Energy Research Establishment,
HARWELL.

June 1966.

HL 66/3531 (C15)

MS

CONTENTS

TABLES

ILLUSTRATIONS

ILLUSTRATIONS (Cont'd.)

Figure

1. Introduction

Inert gas atoms are produced in some materials by neutron irradiation. The low solubility of the inert gases in most solids (Rimmer and Cottrell, 1957) can lead to agglomeration of the gas atoms with the eventual formation of bubbles. Such bubbles have been observed directly by transmission electron microscopy in uranium (Hudson, 1965), uranium dioxide (Whapham, 1965) and beryllium oxide (Woollaston and Wilks, 1964). In addition the formation and subsequent thermal behaviour of bubbles in solids has been studied extensively in the electron microscope after introducing inert gas atoms in thin foils with an ion accelerator (Barnes 1960, Barnes and Mazey 1963).

In neutron-irradiated magnesium oxide, transmutation of the naturally occurring isotopes of magnesium and oxygen produces neon and helium (e.g. Everling et al, 1961). No evidence for bubble formation has been reported previously in magnesium oxide, although Bowen and Clarke (1964) observed small defect clusters by transmission electron microscopy after irradiation to a dose of 4.3×10^{20} nvt* and subsequent annealing at 1,500°C. In the present work crystallographically oriented bubbles have been found after annealing at higher temperatures and this paper describes their appearance and characteristics over a range of doses.

Electron microscope observations have also been carried out in conjunction with the gas release studies of Scott and Wassell (1966). There is an extensive literature on the mechanisms of gaseous transport and release in solids including the role of irradiation-induced defects, but there appear to have been few experiments in which such mechanisms have been related to the direct observation of defects by transmission electron microscopy. In the present work this approach has enabled the form of the release curve obtained by crushing the specimen to be interpreted in terms of dislocations and bubbles.

2. Experimental

Magnesium oxide single crystals obtained from Semi-Elements Inc., Saxonburgh, Pa., were irradiated in the Harwell DIDO and PLUTO reactors to doses ranging from 6×10^{19} to 8.8×10^{20} nvt, at 150°C, 600°C and 1,000°C. The total impurity content of the crystals was typically about 500 ppm, the major impurities being Ca, Al, Fe and Si.

Annealing treatments were in an argon atmosphere; care was taken to ensure that heating and cooling times were short compared with the quoted periods for which the specimens were held at temperature. Annealed crystals

---

*All doses are quoted for neutron energies $\geq$ 1 MeV.

were cleaved into {100} flakes 0.1 mm thick and these were further reduced by chemical polishing to ~2,000 Å to permit examination in a JEM 6A electron microscope. Except where otherwise stated, the plane of observation was close to {100}. In cases where the density of defects was determined from micrographs, the thickness of the specimen was estimated from slip traces introduced by plastic deformation during preparation; these could readily be distinguished from dislocations resulting from irradiation damage.

Gas release studies were carried out by two methods, thermal release and mechanical release. A detailed account of the apparatus and measurements has been given by Scott and Wassell (1966) and the methods are described only briefly here. The apparatus consisted of a high vacuum system coupled to a mass spectrometer and thermal release was achieved by induction heating in a vitreous carbon crucible. Mechanical release was achieved at room temperature by crushing the specimen with a reciprocating plunger in an evacuated steel vessel. The quantity of gas released was measured by communicating this vessel with a known volume in the mass spectrometer and observing the resultant pressure.

Dimensional changes were measured on 2.5 cm long bars with lapped end-faces, using a comparator accurate to better than 10^{-5} cm.

3. Electron Microscopy

In all specimens that had been annealed, dislocation loops and tangles were observed as previously described by Groves and Kelly (1963) and Bowen and Clarke (1964). In addition, for doses > 10^{20} nvt, specimens that had been annealed above 1,500°C showed the presence of rectilinear defects as illustrated in Figure 1(a). No such defects were observed in 'as-irradiated' or in unirradiated, annealed crystals. The defects faded in and out of contrast on tilting the specimen and showed light or dark contrast depending on the diffracting conditions and on their depth in the foil. The sides of the defects were along <100> and the ratio of the lengths of their sides varied between 1.0 and 1.25. No line images were found as would be the case if the defects were {100} platelets; from this and observations on foils tilted through 45° it was concluded that the defects were approximately cubic in shape. Some of the defects were associated with dislocations (Figure 1(b)) where they usually showed a reversal in contrast, and they were frequently located at cusps in the dislocation lines. Evidence will be presented later in the paper suggesting that the defects formed initially as cavities into which Ne and He subsequently diffused. For simplicity they are henceforth referred to as bubbles except when discussing their mode of formation.

Observations of bubbles over a range of doses, irradiation temperatures and annealing temperatures are summarised in Table 1. Annealing at 1,500°C gave variable results. In two anneals, of 1 and 10 hours respectively, no bubbles were found; in another, bubbles of indeterminate shape were observed (No. 4 of Table 1) while in a fourth anneal of 1 hour there was a small number of rectilinear bubbles. Rectilinear bubbles were invariably observed after annealing for 1 hour at 1,600°C and above. It is probable that bubble formation was sensitive to slight differences in annealing conditions close to 1,500°C. Figure 2 shows a size distribution curve, derived from electron micrographs, for bubbles in specimen 7 and curves for other doses had upper and lower limits as shown in Table 1; no systematic variation of bubble size with dose is apparent. Annealing at 2,000°C and above produced changes in shape of the bubbles without an appreciable change in size. Some bubbles had corners that appeared inclined at 45° to the <100> sides, but it was not possible to determine from the {100} projection employed for microscopy whether these were due to the development of {110} or {111} faces. Some of the foils, previously annealed at 1,800°C, were given pulse anneals in the electron microscope by means of the heating effect of the electron beam, but showed no evidence of migration or coalescence of bubbles in the manner described by Barnes and Mazey (1963, 1964).

A number of foils was examined in dark field using a single diffracted beam alined with the axis of the microscope. Anomalous strain contrast, (Ashby and Brown, 1963) was observed around some of the smaller bubbles (<~100 Å). In all experiments the asymmetry of the image relative to the diffraction vector in reciprocal space was consistent with an inward relaxation of the bubble surface. Such a relaxation is to be expected in the case of a void or a bubble whose internal pressure is insufficient to balance the stresses arising from the surface energy (Nelson et al 1964, Brown and Mazey 1964).

The crystals irradiated to 4×10^{20} nvt at 1,000°C showed features not observed in those irradiated at lower temperatures. The 'as-irradiated' specimens contained precipitates 1,000 to 2,000 Å in size, many of which had acted as dislocation sources (Figure 3). Magnesium oxide crystals frequently contain precipitates (Venables 1963, Henderson 1964) but in this particular crystal they were larger than before irradiation and it is assumed that they had grown during the irradiation period of approximately one year at 1,000°C. The dislocations associated with the precipitates in Figure 3 were presumably generated by differential thermal contraction on cooling to room temperature. Examination in the ultramicroscope showed that many of the precipitates were also associated with the 'grown-in' dislocation network of the crystal including sub-grain boundaries.

TABLE 1

Characteristics of bubbles in neutron irradiated MgO

	Dose (nvt)	Irradiation Temperature °C	Annealing Temperature °C	Annealing Time Minutes	Bubbles			Remarks
					Density cm^{-3}	Size Å	Shape	
1	Unirradiated	-	1800	60	-	-	-	No bubbles observed
2	6×10^{19}	150	1800	60	-	-	-	No bubbles observed
3	10^{20}	150	1800	60			Rectilinear	
4	4.3×10^{20}	150	1500	60	4.7×10^{14}	50	Indeterminate	
5	4.3×10^{20}	150	1600	60			Rectilinear	
6	4.3×10^{20}	150	1700	60		40-240	Rectilinear	
7	4.3×10^{20}	150	1800	60	4.1×10^{14}	50-300*	Rectilinear	*See figure 2
8	6.5×10^{20}	150	1800	60		60-360	Rectilinear	
9	6.5×10^{20}	150	2000	60		85-400	Straight sides but with rounded or 45° corners	
10	6.5×10^{20}	150	2300	30		300	Polyhedral or spherical	
11	6.5×10^{20}	150	1800	0.25	-	-	-	No bubbles observed
12	6.5×10^{20}	150	1800	0.5		40-160	Rectilinear	
13	6.5×10^{20}	150	1800	1		30-130	Rectilinear	
14	6.5×10^{20}	150	1800	5	1.3×10^{14}	50-180	Rectilinear	
15	8.8×10^{20}	150	1600	60		50-200	Rectilinear	
16	8.8×10^{20}	150	1800	60	6.4×10^{14}	40-340	Rectilinear	
17	4.0×10^{20}	600	1800	60		100-250	Rectilinear	
18	4.0×10^{20}	1000	1800	60	4×10^{9}†	300-2000	Rectilinear and polyhedral	†Determined from an optical micrograph.

After annealing for one hour at 1,800°C, however, no precipitates were observed, but the specimens contained bubbles ranging in size from 300 to 2,000 Å. The larger bubbles were visible in the ultramicroscope and it was evident that, like the precipitates in the unannealed material, many had formed at sub-grain boundaries. The large bubbles were sometimes polyhedral (Figure 4(a)) or had rounded corners and were usually associated with dislocations (Figure 4(b)).

4. Gas Release

4.1 Thermal Release

The gas released from a specimen irradiated to 6.5×10^{20} nvt was compared with that released from a similar dose specimen give a post-irradiation anneal of 1 hour at 1,700°C. The results of Scott and Wassell (1966) showed that evolution of detectable amounts of both neon and helium occurred in both specimens above 1,500°C and became extremely rapid above 1,770°C consequent upon dissociation of the MgO. The release from the pre-annealed specimen, however, was about three times as great as that from the 'as-irradiated' specimen. The measurements were carried out under dynamic pumping conditions and suggested that helium was being evolved from the specimens at a greater rate than neon.

4.2 Mechanical Release After Isochronal Annealing

Specimens irradiated at 150°C and 1,000°C respectively were annealed for one hour at various temperatures between 700°C and 1,950°C, and the quantity of gas released by crushing at room temperature was measured. The results for helium are shown in Figure 5. Release of neon showed similar behaviour, but the quantity evolved from annealed specimens was an order of magnitude lower than for helium. The amounts of helium and neon released from unannealed specimens, however, were comparable.

4.3 Mechanical Release After Isothermal Annealing

Experiments were carried out at two doses, 6×10^{19} nvt and 6.5×10^{20} nvt, the irradiation temperature being 150°C. Samples for gas release and electron microscopy from each dose were annealed at 1,800°C for times ranging from five seconds to two hours. Gas release curves obtained by crushing at room temperature are shown in Figure 6. Details of the formation of bubbles are given in Table 1 (numbers 2 and 11-14) and dislocation densities, determined from the micrographs, are shown in Figure 7 for the higher dose. The annealing sequence of the dislocations is illustrated in Figure 8 and was similar at the lower dose. To determine whether the particle size

after crushing changed significantly as a function of annealing time, surface areas of some of the powdered specimens were measured by a ^{85}Kr adsorption method (Aylmore and Jepson 1961). The results are shown in Table 2.

Table 2

Surface areas of crushed specimens

Dose nvt $\geq$ 1 MeV	Heat treatment	Mass of crushed sample (gm)	Mean surface area per gm (cm^2)
6.5×10^{20}	As-irradiated	0.1340	$1.73 \times 10^4 \pm 0.17$
6.5×10^{20}	10 min. at 1800°C	0.1046	$1.96 \times 10^4 \pm 0.20$
6.5×10^{20}	120 min. at 1800°C	0.0840	$1.17 \times 10^4 \pm 0.12$
Unirradiated	None	0.1224	$2.53 \times 10^4 \pm 0.25$

The crushed crystals were also examined by optical and electron microscopy; the particle sizes ranged from ~100 Å to ~10 μm and the size distribution appeared similar for both annealed and unannealed crystals.

5. Macroscopic Growth

The total bubble volume per unit volume of crystal, calculated from the size distribution curve for number 7 of Table 1, is compared in Table 3 with the residual volume change $\Delta V/V$, determined from macroscopic growth measurements for the same dose and annealing temperature.

Table 3

Comparison of total bubble volume and macroscopic volume expansion after annealing at 1800°C

Dose nvt	Annealing Temperature °C	Total bubble volume per cm^3 of MgO	$\Delta V/V$ from macroscopic growth
4.3×10^{20}	1800	2.4×10^{-3}	2.2×10^{-3}

6. Gas Production

Under neutron irradiation the following reactions can occur in magnesium oxide (Everling et al., 1961).

$$Mg^{24} + n \longrightarrow Ne^{21} + He^{4}$$
$$Mg^{25} + n \longrightarrow Ne^{22} + He^{4}$$
$$Mg^{26} + n \longrightarrow Ne^{23} + He^{4}$$
$$Ne^{23} \longrightarrow Na^{23} + \beta$$
$$O^{16} + n \longrightarrow C^{13} + He^{4}$$

The helium concentration for a dose of 6.5×10^{20} nvt has been determined experimentally by Scott and Wassell (1966). Calculations (Wilks 1966) based on computed cross-sections, give a value reasonably consistant with the experimental result and indicate that the neon concentration is about half that of helium. On this basis, the total gas content per unit volume of magnesium oxide, making use of Scott and Wassell's result, would be 2.1×10^{-2} cm^3 (at NTP) for a dose of 4.3×10^{20} nvt. Using the value for the bubble volume in Table 2, the mean bubble pressure would not exceed ~10 atm, even if all the gas had accumulated in the bubbles during annealing.

7. Correlation of Gas Release Results and Electron Microscope Observations

Dealing first with Figure 6, it appears unlikely, from Table 2, that the main features of curve (a) can be explained simply by differences in crushing behaviour. In the work of MacEwan and Stevens (1964) on the release of inert gases from crushed, polycrystalline UO_2, the results were interpreted in terms of gas trapped in pores and in irradiation-induced vacancy clusters. For the single crystals used in the present work a qualitative explanation of the form of the curves in Figure 6 can be advanced involving the release of gas from two kinds of irradiation-induced trapping sites, dislocations and bubbles. In this discussion, the curves are considered in two stages; first, the pronounced peak after short annealing periods and second, the approximately linear portions after longer annealing times.

Of the defects considered, the initially high density of dislocations suggests that the peaks in Figure 6 result primarily from the gas associated with dislocations. The quantity of gas released will be proportional to the amount of gas associated with unit length of dislocation line, the fraction of the total length of dislocations intersected by the new surface created on crushing and the rate of gaseous transport to the surface. The latter could occur in two ways, by diffusion or by movement of the dislocations together with their atmospheres to the surface under the influence of the stresses created by crushing. Information on the rate of

gaseous diffusion in oxide ceramics, including MgO, has been given by Morrison et al. (1964) for ^{18}O and ^{133}Xe between 700 and 1500°C. Extrapolation of their data to room temperature indicates that, unless the diffusion coefficients for Ne and He are greater by many orders of magnitude, the release of gas at bulk diffusion rates during the time of the crushing experiment would be negligible compared to the relatively large fractional release observed. (Figure 6). This release could be explained, however, on the assumption that pipe diffusion along dislocation cores is a more rapid process than bulk diffusion. Rovner (1966) has recently found evidence for pipe diffusion of oxygen in a crushed MgO single crystal at 750°C at a rate $\sim 5 \times 10^{10}$ greater than for lattice diffusion. Supporting evidence for the transport of inert gases by pipe diffusion, however, is somewhat inconclusive. The possibility was considered by Hasiguti and Igata (1962) for the diffusion of fission gases in uranium and Lagerwall (1964) has suggested that Ar in CaF_2 moves by this mechanism. On the other hand, Barnes and Mazey (1963) found no evidence for pipe diffusion between helium bubbles associated with dislocations in copper. Such a process may be more favourable in ionic solids than in metals because of the relatively large size of the dislocation cores (Love, 1965).

With regard to dislocation movement, it is known that slip can occur at room temperature in unirradiated MgO and that interstitial dislocation loops form on the $\{110\}$ slip planes during post-irradiation annealing. (Groves and Kelly 1963, Bowen and Clarke 1964). Glide therefore appears to be a possible means of escape for the dislocation atmospheres although pinning by other irradiation-induced defects (Clarke and Sambell 1960, Sambell and Bradley 1964) and by impurities (Stokes 1965) makes it difficult to assess the ease with which this process could occur. A similar hypothesis has been proposed by Morgan et al. (1965) to account for the enhanced release of gas from fissile oxides on application of a compressive stress.

The peaks in Figure 6 presumably result from a balance between a number of conflicting factors of which the most important are the increasing concentration with time of inert gas atoms at the dislocations and the decrease in dislocation density as illustrated in Figure 7. An additional factor is the change in the configuration of the dislocations as shown in Figure 8. Initially (Figure 8(a)), a large number of dislocations are in the form of multiply-connected loops which, at later stages in the annealing, grow in size (Figure 8(b)) and appear to become less tangled. This process, coupled with progressive annealing of point defects, would increase the ease with which slip could occur and could also result in an increasing proportion of the total length of dislocation line being connected to the surface on crushing, thereby favouring either or both of the

release mechanisms discussed above. Ultimately, these processes will be countered by the fall in dislocation density (Figures 7, 8(c)), leading to a decrease in the quantity of gas released.

Annealing out of the dislocations will leave their gas atmospheres free to diffuse to other sinks in the crystals. In the higher dose crystal, but not the lower, (Figure 6(a) and Table 1) the bubbles provide alternative sinks and accumulation of gas in them could account for the second rise in release in Figure 6(a). Release of this gas takes place by the intersection of a proportion of the bubbles by the new surface created on crushing and the ratio of gas released from a crystal containing bubbles of size 'a' to that released from a crystal without bubbles in which the gas is uniformly distributed will be approximately $1 + \frac{fa}{2\delta}$, $(a>>\delta)$, where δ is the thickness of crystal from which gas is released by cleaving and f is the fraction of gas in the bubbles. Table 1 shows that 'a' is approximately constant for the bubbles observed in the present work and the rise in the release curve results principally from the increase in f as more gas diffuses to the bubbles.

The curves in Figure 5 show that the quantity of gas released on crushing increases rapidly for annealing temperatures above 1500°C, at which bubble formation is observed. Assuming that δ, at room temperature, is of atomic dimensions, gas release ratios similar to those determined from Figure 5 can be obtained by varying f between 0 and 1, using typical bubble sizes (Table 1). It might be expected that the high dislocation content of the specimens after annealing in the range 1000-1500°C (Bowen and Clarke, 1964) would give rise to a release peak in a similar manner to that discussed for Figure 6, particularly for the crystal irradiated at 150°C. The absence of such a peak, however, is consistent with the view that vacancy mobility is too low at temperatures below 1500°C for gas atoms, which are generally considered to diffuse by a vacancy mechanism, to form sufficiently high concentrations around dislocations.

The results of the thermal release experiment were complicated by the rapid dissociation of MgO at high temperatures under vacuum (Livey and Murray, 1956). It is significant, however, that appreciable gas release did not occur until above 1500°C, lending further support of the view that the rate of diffusion of neon and helium is linked with the temperature at which vacancy mobility becomes appreciable.

8. Mechanism of Bubble Formation

As discussed by Greenwood et al. (1958) and Nelson et al. (1964) a bubble is thermodynamically stable only when the gas pressure in it is sufficient to exactly balance the inward force created by the surface tension. Nelson et al. have shown that for a cubical bubble to be stable

the internal pressure p must equal $\frac{4\gamma}{a}$ where γ is the surface energy and 'a' is the length of a side. For cubical bubbles of side 180 Å and $\gamma_{\{100\}}$ = 1150 erg cm^{-2} (Westwood and Goldheim 1963) the equilibrium pressure would be 2,550 atm (assuming that the surface tension equals the surface energy). In the present study the quantity of gas generated in the crystal appears insufficient to create pressures two orders of magnitude below this (Section 6).

At 1800°C, bubbles become evident after 30 seconds yet they do not form below 1500°C even during long anneals. When they are formed above this temperature their sizes all fall within the range 40-400 Å. These facts, together with the evidence that gas continues to accumulate in the bubbles long after their time of formation (Figure 6(a)) suggest that initially, cubical cavities (containing only a nominal number of gas atoms) are formed by vacancy condensation, but that a certain minimum concentration of mobile vacancies is required for the process to take place. At doses below 10^{20} nvt, the vacancy supersaturation is too low and at temperatures below 1500°C the vacancy mobility is too low for cavity formation to occur. A high vacancy concentration is to be expected because of the interstitial character of dislocation loops in neutron irradiated MgO (Groves and Kelly 1963, Bowen and Clarke 1964). It is significant that the bubble volume deduced from electron micrographs agrees closely with the directly measured growth (Table 2), since an ion in an interstitial loop together with its corresponding vacancy forming part of a cavity can be regarded as contributing one atomic volume to the macroscopic volume expansion of the crystal. As bubbles form, the vacancy supersaturation would be rapidly dissipated and further vacancy movement might be expected to result in a contraction of the bubble volume owing to surface energy effects. However, this appears to be very slow process in single crystals and was not evident in the present studies at temperatures below 2000°C.

Rectilinear cavities or bubbles with {100} surfaces have also been observed in neutron irradiated LiF (Gilman and Johnston, 1958) and KI, KBr and KCl (Budylin and Kozlov, 1964) after annealing. In each case the authors concluded that any gas in the cavities was at low pressure and that they were formed by condensation of vacancies arising from the liberation of free halogen atoms during irradiation.

The equilibrium shape of a particle or cavity has been discussed by Herring (1953) in terms of the variation of surface energy with the orientation of crystallographic planes. Cavities would be expected to form with {100} sides in MgO since this material exhibits {100} cleavage suggesting that these planes have minimum surface energy. At high temperatures (>2000°C), however, the bubble shapes change, suggesting that the relative

values of surface energy on {100}, {110} and possibly {111} planes are changing with temperature. In the crystal irradiated at 1000°C it is thought that the large bubbles present after annealing at 1800°C result from dissolution of the precipitates in the matrix to create cavities into which gases subsequently diffuse. Surface energies are known to depend sensitively on contamination and the polyhedral shapes observed may result from the presence of a high concentration of impurities.

Acknowledgements

We are indebted to Dr. K. T. Scott and Mr. L. Wassell for their collaboration, to Mr. N. Mattingley for his careful preparation and help with the electron microscopy, to Mr. J. A. G. Smith for macroscopic growth measurements and to Dr. J. K. Higgins for the surface area determinations. We wish to thank Drs. R. S. Nelson and A. J. E. Foreman for useful discussions and Drs. F. J. P. Clarke and J. Williams for their general support and helpful comments on the manuscript.

References

Ashby, M. F. and Brown, L. M., 1963. Phil. Mag. 8, 1083, and 1649.

Aylmore, D. W. and Jepson, W. B. 1961. J. Sci. Inst. 38, 156.

Barnes, R. S., 1960, Phil. Mag. 5, 635.

Barnes, R. S. and Mazey, D. J., 1963. Proc. Roy. Soc. A. 275, 47.

1964. Proceedings, Third European Regional Conference on Electron Microscopy. Czechoslovak Academy of Sciences, Prague, p. 197.

Bowen, D. H. and Clarke, F. J. P., 1964. Phil. Mag. 9, 413.

Brown, L. M. and Mazey, D. J., 1964. Phil. Mag. 10, 1081.

Budylin, B. V. and Kozlov, Yu, F., 1964. Fizika Tverdogo Tela 6, 1573.
Soviet Physics - Solid State, 6, 1237.

Clarke, F. J. P. and Sambell, R. A. J., 1960. Phil. Mag. 5, 697.

Everling, F., Koenig, L. A., Mattauch, J. H. E. and Wapstra, A. H., 1960. Nuclear Data Tables. Part 1. U.S.A.E.C.

Gilman, J. J. and Johnston, W. G., 1958. J. Appl. Phys. 29, 877.

Greenwood, G. W., Foreman, A. J. E. and Rimmer, D. E., 1959., J. Nucl. Materials, 4, 305.

Groves, G. W. and Kelly, A., 1963. Phil. Mag. 8, 1437.

Hasiguti, R. R. and Igata, H., 1962. "Properties of Reactor Materials and the Effect of Radiation Damage", p.527. Ed. D. J. Littler, London, Butterworths.

Henderson, B., 1964. Phil. Mag. 9, 153.

Herring, C., 1953, "Structure and Properties of Solid Surfaces", Ch. 1, Eds. R. Gomer and C. S. Smith. University of Chicago Press.

Hudson, B., 1965. Private communication.

Lagerwall, T., 1964. Nucleonik, 6, 179.

Livey, D. T. and Murray, P., 1956. J. Nucl. Energy, 2, 202.

Love, G. R., 1965. Private communication.

MacEwan, J. R. and Stevens, W. H. 1964. J. Nucl. Materials 11, 77.

Morgan, C. S., Fitts, R. B. and Scott, J. L. 1965. J. Am. Ceram. Soc. 48, 166.

Nelson, R. S., Mazey, D. J. and Barnes, R. S., 1965. Phil. Mag. 11, 91.

Rimmer, D. E. and Cottrell, A. H., 1957. Phil. Mag. 2, 1345.

Rovner, L. H., 1966. Technical Report No. 10., Department of Engineering Physics, Cornell University, Ithaca, New York.

Sambell, R. A. J. and Bradley, R., 1964. Phil. Mag. 9, 161.

Scott, K. T. and Wassell, L., 1966. To be published.

Stokes, R. J., 1965. J. Am. Seram. Soc. 48, 60.

Venables, J. D., 1963. J. Appl. Phys., 34, 293.

Westwood, A. R. C. and Goldheim, D. L., 1963. J. Appl. Phys. 34, 3335.

Whapham, A. D., 1965. Trans. Am. Nucl. Soc. 8, No. 1, 21.

Wilks, R. S., 1966. J. Nucl. Materials. To be published.

Woollaston, H. J. and Wilks, R. S., 1964. J. Nucl. Materials, 12, 305.

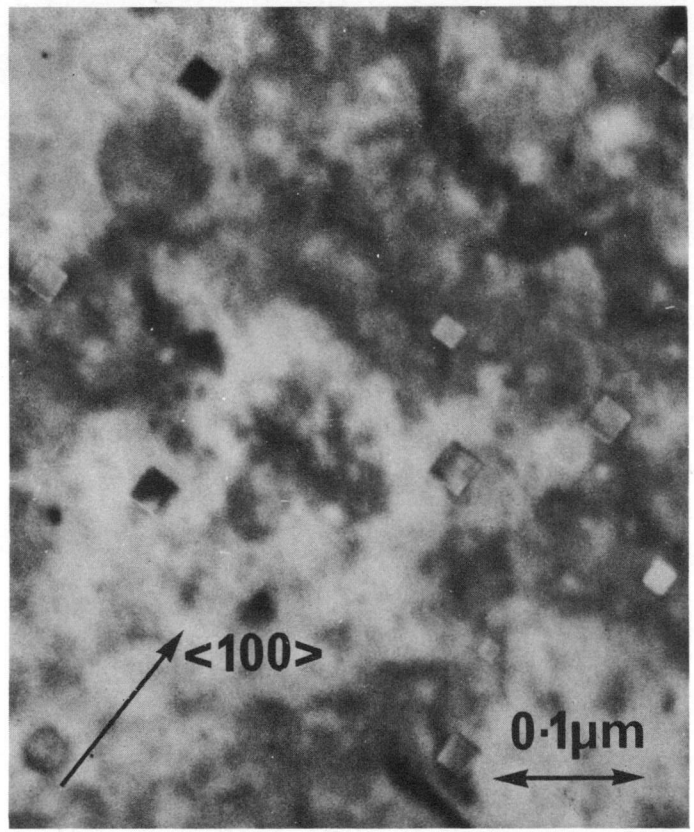

AERE - R 5223 Fig. 1(a)
Rectilinear defects showing light and dark contrast. Dose 6.5 x 10^{20} nvt.
Annealed for 1 hour at 1800°C.

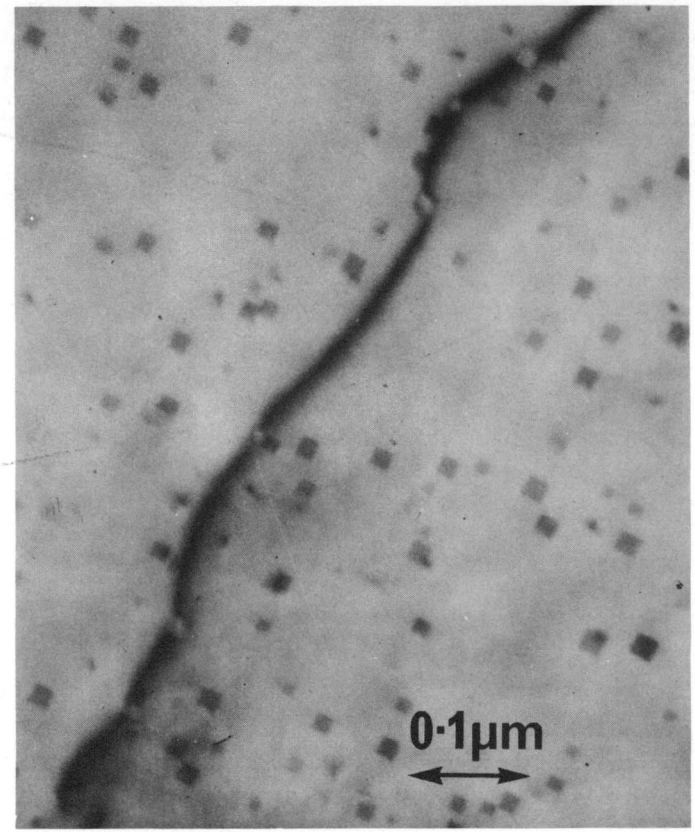

AERE - R 5223 Fig. 1(b)
Rectilinear defects associated with a dislocation. Dose 4.3 x 10^{20} nvt.
Annealed for 1 hour at 1800°C.

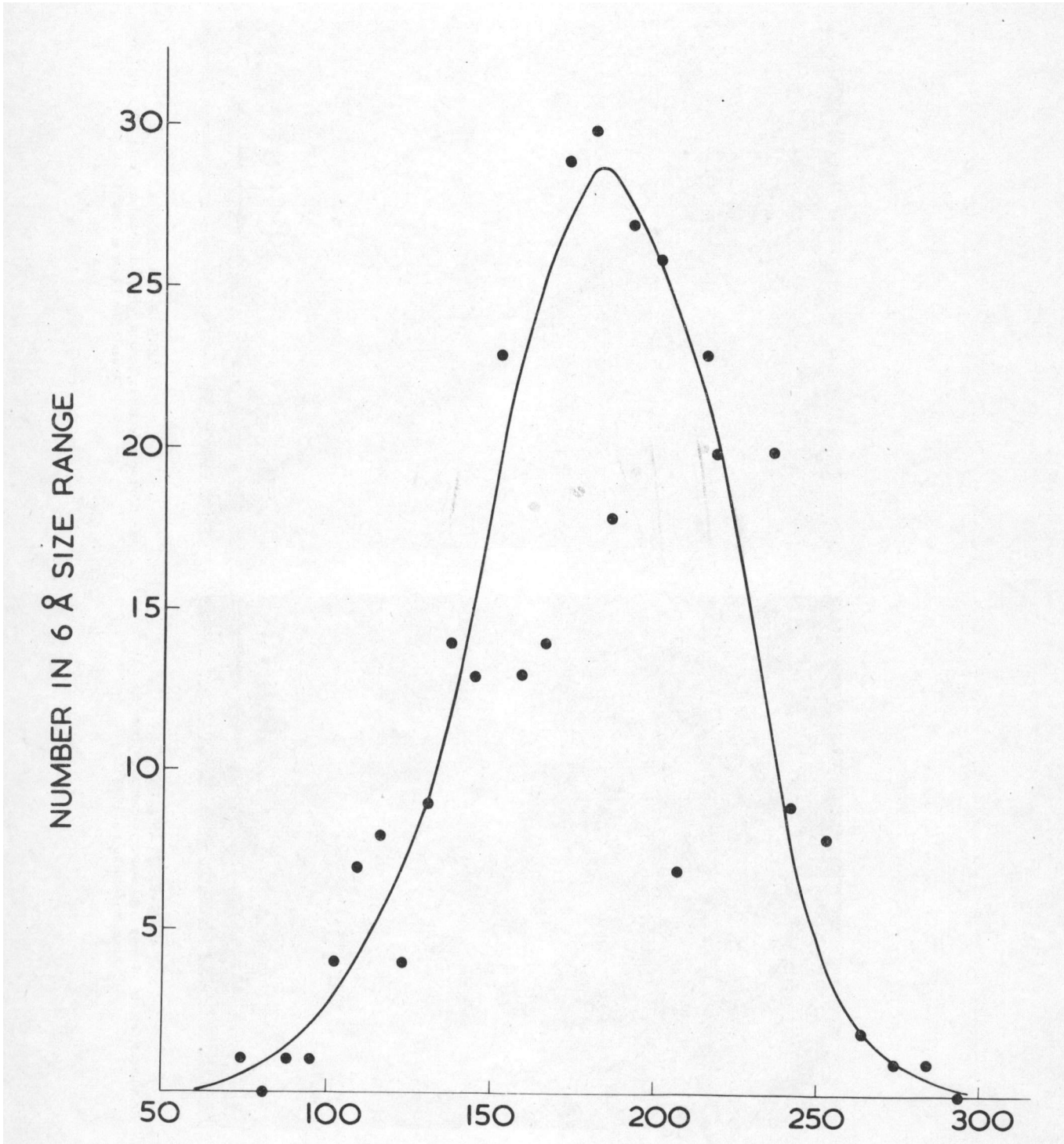

AERE - R 5223 Fig. 2
Size distribution of bubbles for specimen shown in Figure 1(b)

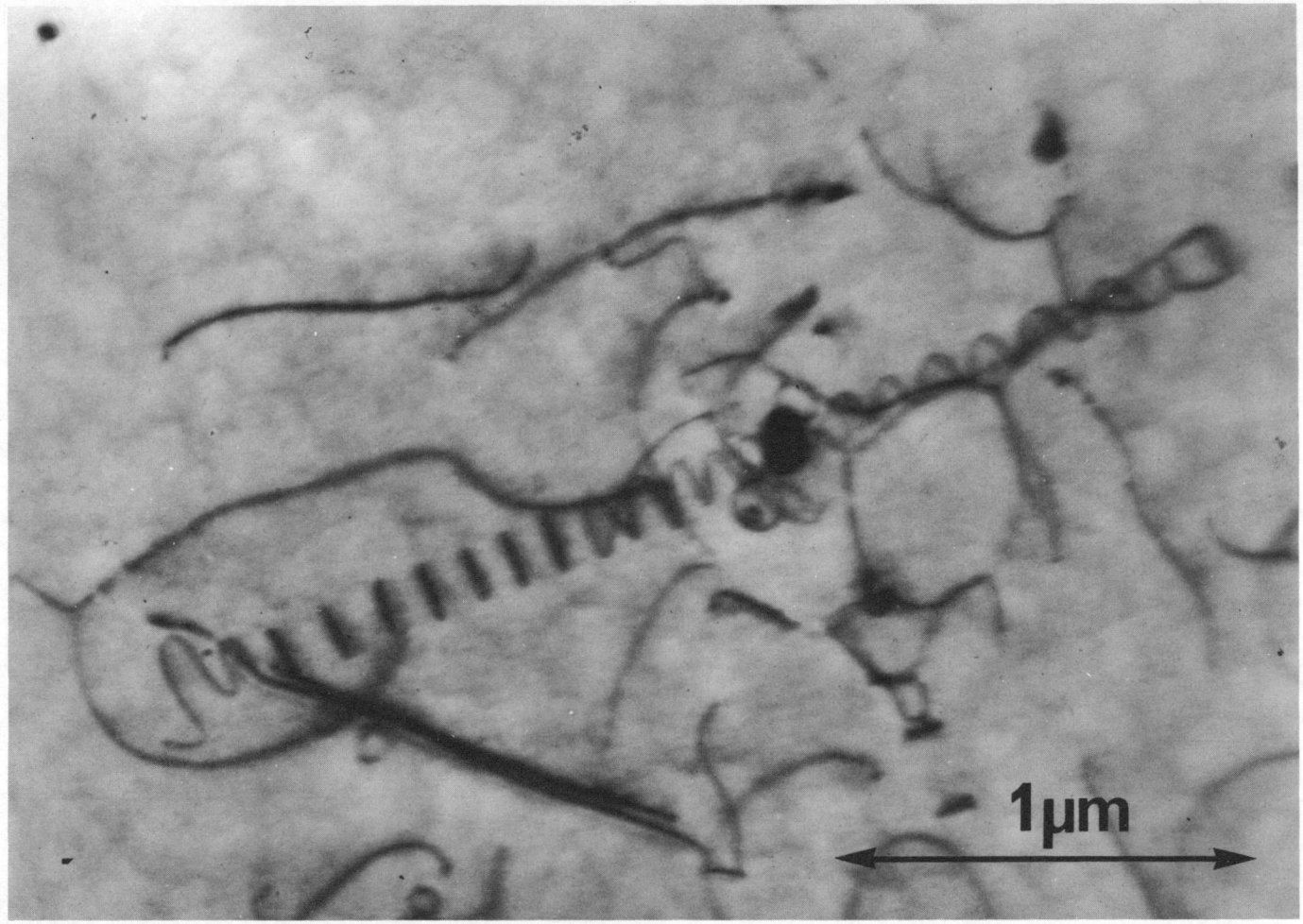

AERE - R 5223 Fig. 3
Prismatic dislocation loops generated by a precipitate in a crystal irradiated at 1000°C.
Dose 4.0 x 10^{20} nvt.

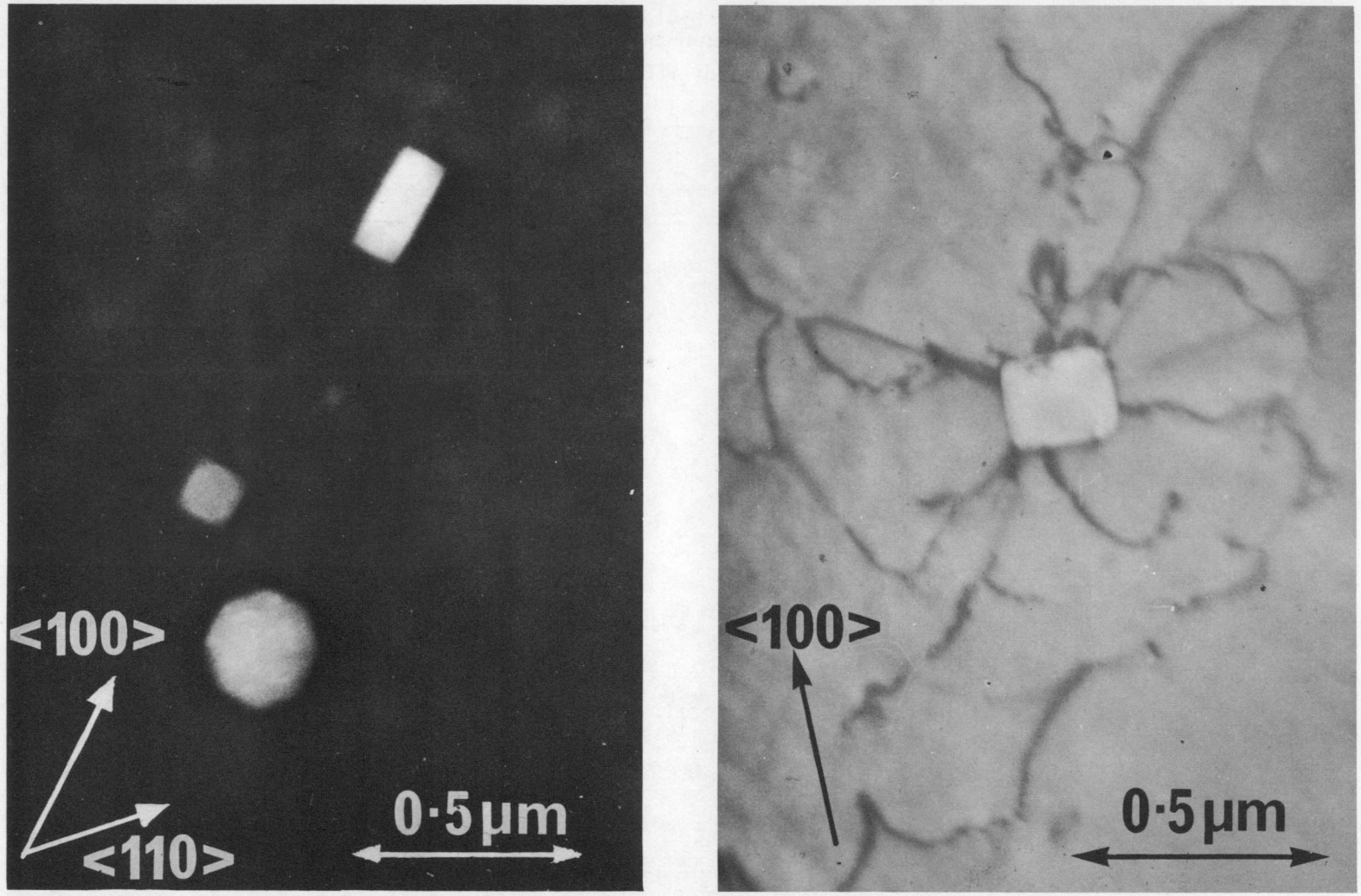

(a) (b)

AERE - R 5223 Fig. 4

Crystal irradiated to 4.0 x 10^{20} nvt at 1000°C and annealed for 1 hour at 1800°C.

(a) Illustrating some of the bubble shapes.
(b) A large bubble associated with dislocations.

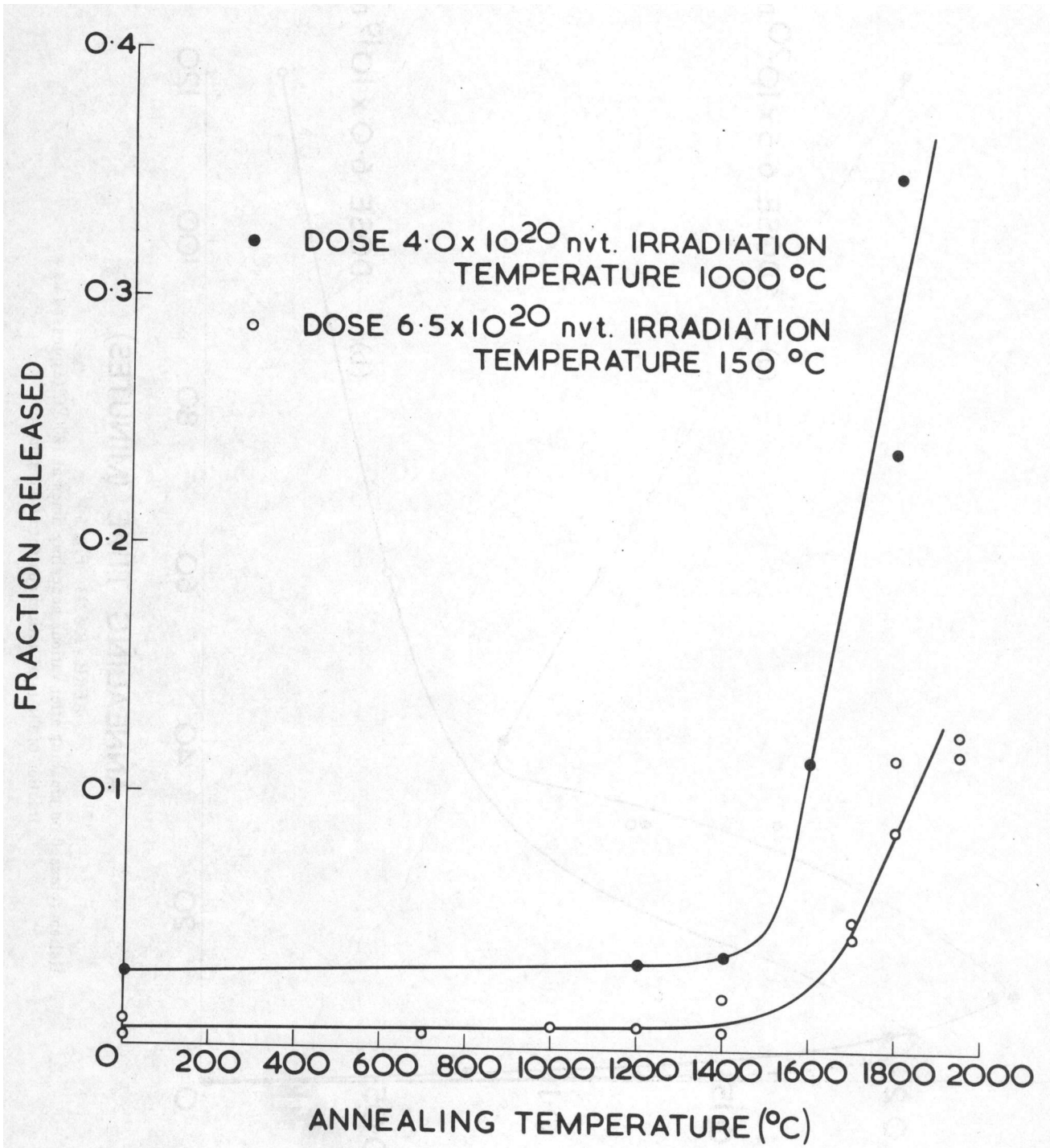

AERE - R 5223 Fig. 5
Helium released on crushing after 1 hour anneals at various temperatures (expressed as a fraction of the total helium content of the sample)

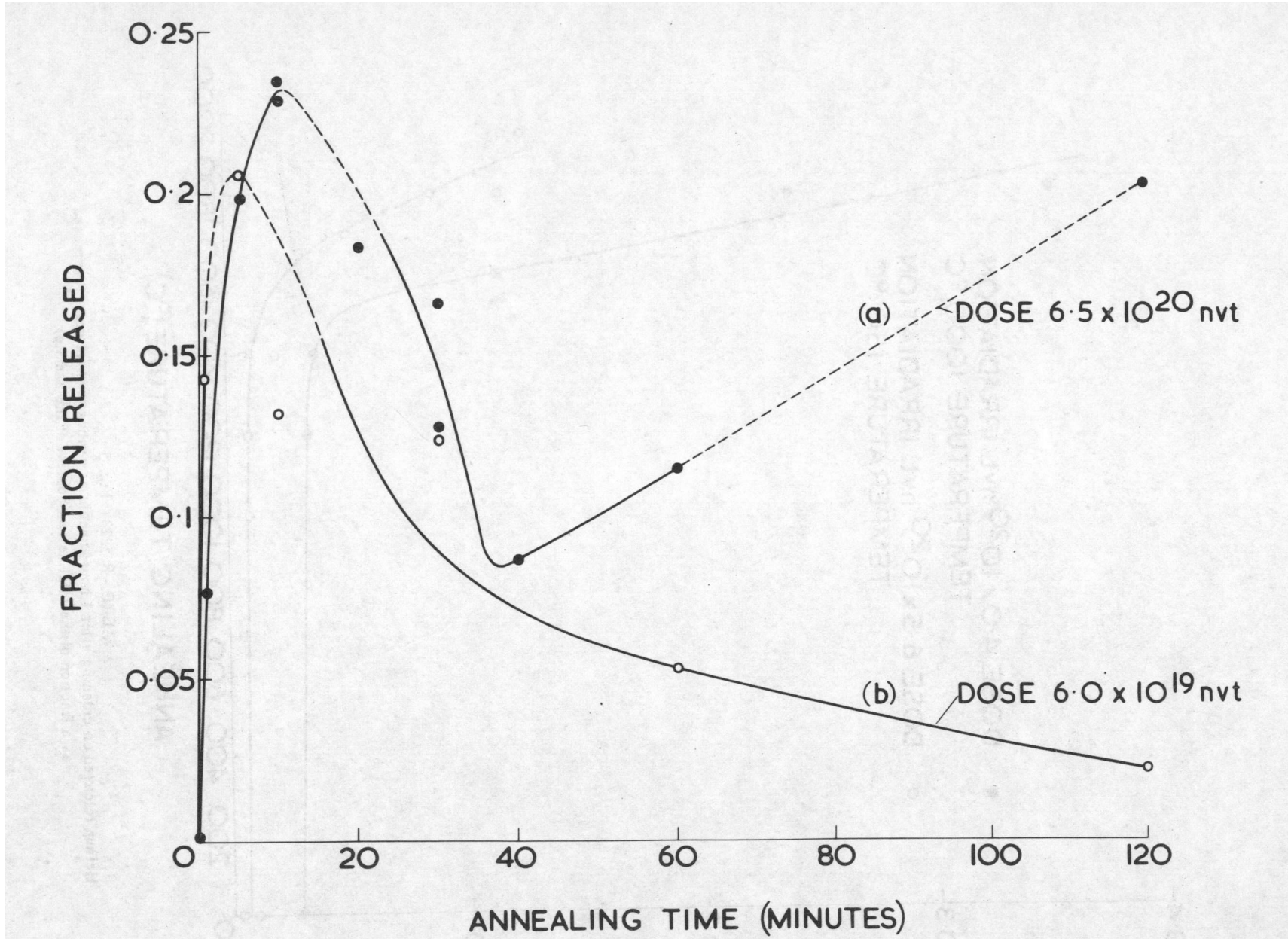

AERE - R 5223 Fig. 6

Helium released on crushing after various annealing times at 1800°C (expressed as a fraction of the total helium content of the sample)

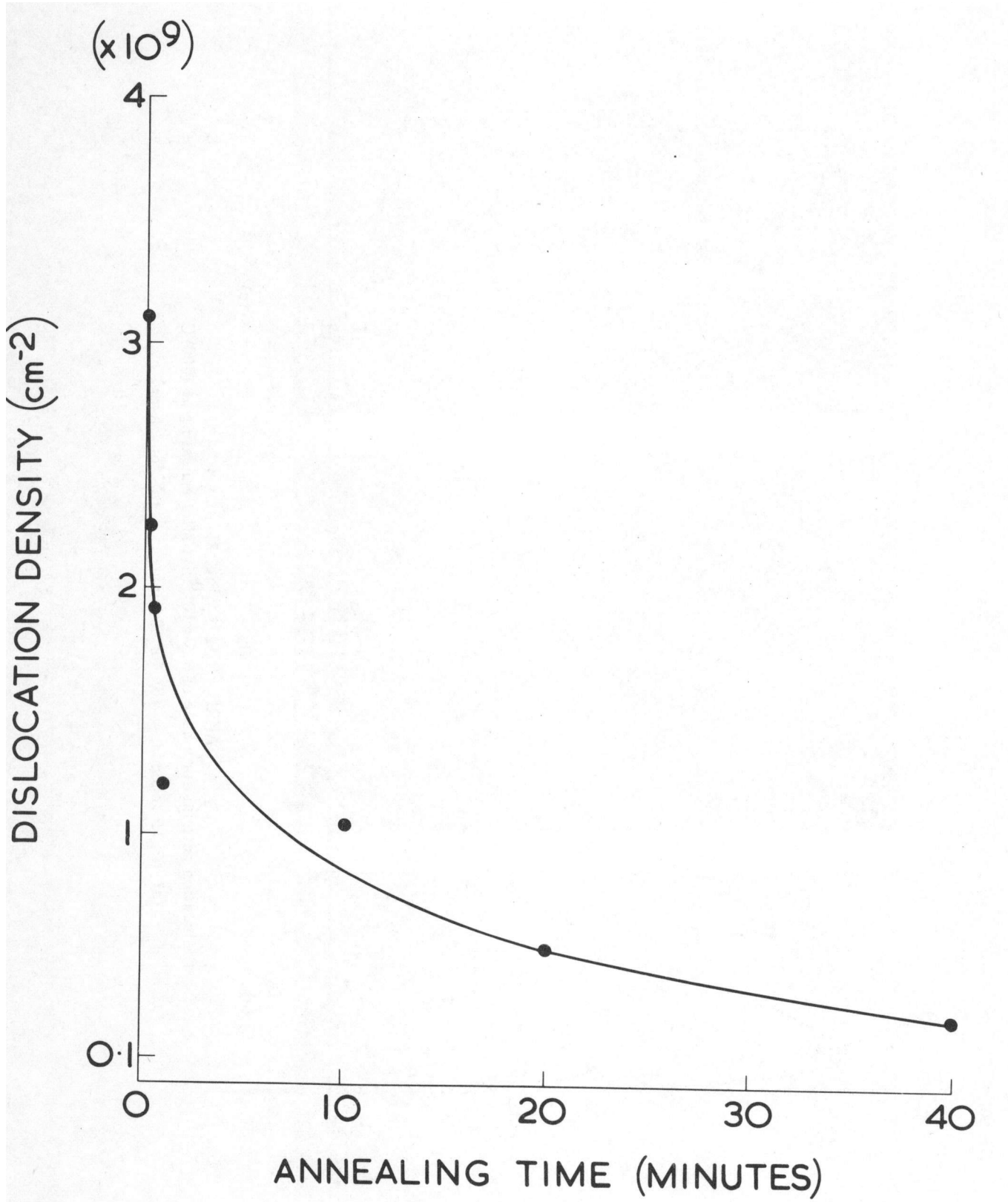

AERE - R 5223 Fig. 7

Variation of dislocation density with annealing time at 1800°C for a dose of 6.5×10^{20} nvt

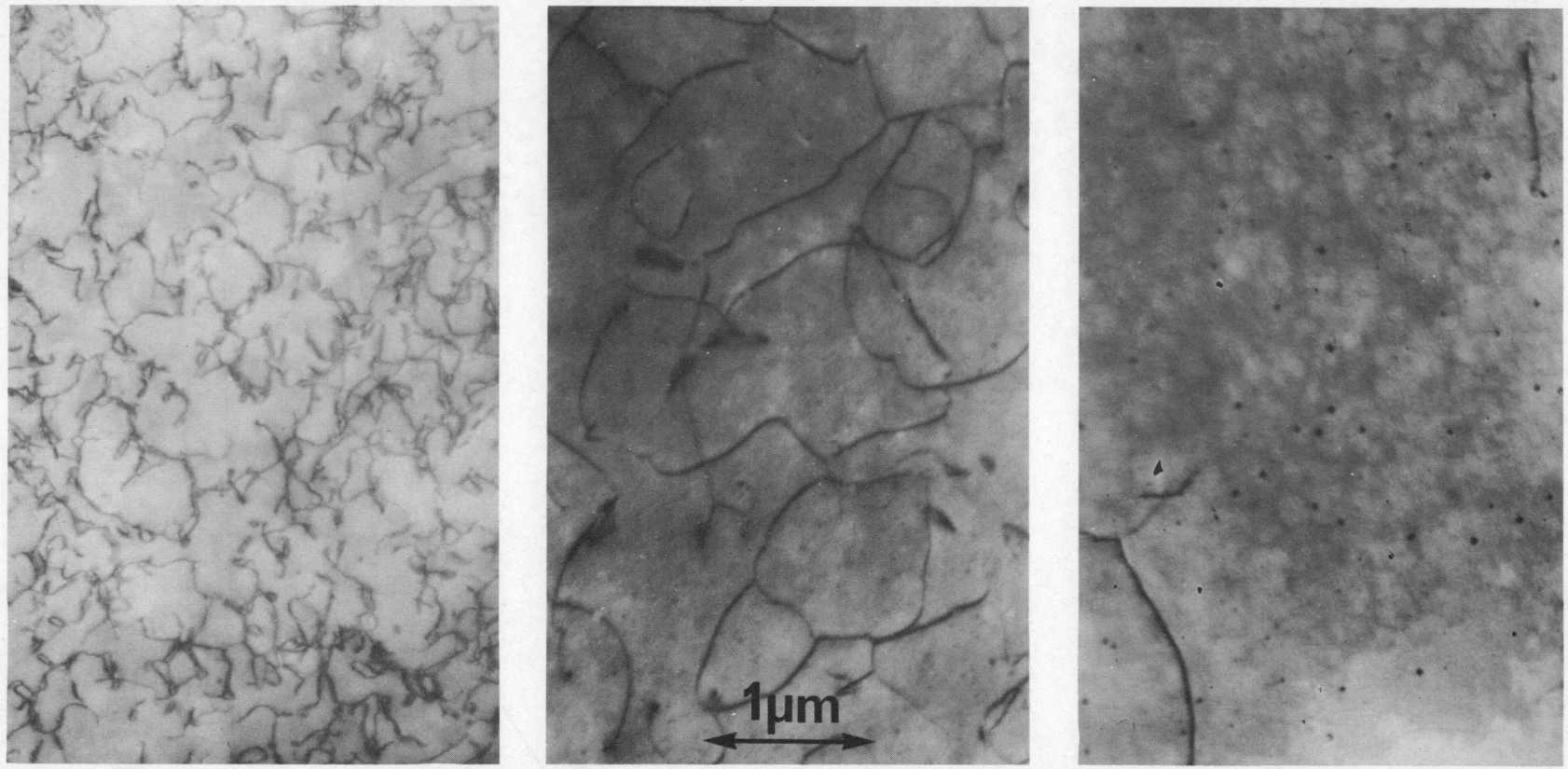

(a) (b) (c)

AERE - R 5223 Fig. 8

Dislocation patterns for a dose of 6.5×10^{20} nvt after annealing at 1800°C

(a) for 15 seconds; (b) for 10 minutes; (c) for 1 hour